Titan Interaction with Saturn's Magnetosphere: Voyager 1 Results Revisited

E. C. Sittler Jr.[1], R. E. Hartle[1], A. F. Viñas[1] , R. E. Johnson[2], H. T. Smith[2] and I. Mueller-Wodard[3]

1. NASA/Goddard Space Flight Center, Greenbelt, MD, 20771, USA, Email: edward.c.sittler@nasa.gov, richard.e.hartle@nasa.gov, adolfo.f.vinas@nasa.gov
2. University of Virginia, Engineering Physics, Thornton Hall Room B103, Charlottesville, VA, 22904, USA, Email: rej@virginia.edu
3. Imperial College, London, UK, Email: i.mueller-wodarg@imperial.ac.uk

We investigate the details of Titan's interaction with Saturn's magnetosphere, which includes formation and location of an ionopause, mass loading via ion pickup and the effects of finite gyroradii. We present new interpretations of the Voyager 1 plasma instrument measurements, not addressed by Hartle et al. (1982). Pickup ions H^+ and H_2^+ dominate in the outermost region with respect to Titan's "ionopause", followed by CH_4^+ at intermediate distances and N_2^+ just outside the "ionopause". Mass loading and slowing down of the ambient plasma is observed to increase as the pickup ion mass increases with decreasing radial distance from Titan's ionosphere. H_2 and CH_4 are molecules not originally included in the exosphere of Titan by Hartle and coworkers and the pickup ions of H_2^+ and CH_4^+ are a new feature of our model calculations and should be present in Titan's exospheric region. Therefore, Titan could be an important source of carbon to Saturn's magnetosphere. Finite gyroradius effects are identified in the plasma interaction with Titan's atmosphere, which results in an asymmetric removal of ambient plasma from Titan's exosphere region. The finite gyroradius effects also show that the observed hot keV ion component of the ambient plasma is a heavy ion such as N^+/O^+. A minimum "ionopause" altitude of 4800 km is estimated by a new approach using mass loading.

1.0 Introduction

A new picture of the interaction of Saturn's rotating magnetospheric plasma with Titan's atmosphere emerged from measurements made by instruments onboard Voyager 1 as it flew by Titan on November 12, 1980. Since then a number of the atmosphere, ionosphere and interaction models (Yung et al., 1984; Yung, 1987; Toublanc et al., 1995; Keller et al., 1998) have been developed that encourage further analysis of this data. Consequently, we extend our earlier interpretation of the plasma measurements in an attempt to account for some of the new information embodied in the recent models.

Voyager 1 plasma and field instruments detected a complex interaction with Saturn's outer magnetosphere (Bridge et al. (1981) and Ness et al. (1981)). These initial results were followed by the more comprehensive analysis (Hartle et al. (1982), Ness et al. (1982) and Neubauer et al. (1984)). The upstream parameters are summarized in Table 1. They showed that the sonic Mach number was less than 1, no shock was detected and the magnetometer did not detect an internal magnetic field. The thermal plasma is composed

of H^+ and N^+/O^+, having densities of 0.1 cm^{-3} and 0.2 cm^{-3} and temperatures of 210 eV and 2.9 keV, respectively. The electron's density is $N_e \sim 0.3$ cm^{-3} with a temperature $T_e \sim$ 200 eV. These constituents yield a high kinetic pressure (due primarily to the hot N^+/O^+) relative to that of the observed 5 nT magnetic field, resulting in a plasma beta of about 11. Hartle et al. (1982), showed that ambient N^+/O^+ had gyroradii $r_g > 5000$ km, which are larger than the physical dimensions of Titan, making finite gyro-radius effects an essential feature of the interaction. The analysis by Hartle et al. (1982) demonstrated that the inbound pass was very complex and that pickup ions had been observed. This result was supported by the enhanced levels of wave emissions observed by the Plasma Wave System (PWS) instrument during the inbound approach (Gurnett et al., 1981; Gurnett et al., 1982). Hartle et al. (1982), hereafter referred to as Paper I, modeled the pickup ions by using a ring distribution, which then had to be convoluted with the Plasma Science (PLS) instrument's response (see Bridge et al., 1977 for a description of the instrument). In Paper I the ambient ions were modeled by convected Maxwellians, which were also convolved with the instruments response function. As shown in Paper I the ambient ions can be modeled with a light component (H^+) and a heavy component (N^+/O^+). The identification of heavy ions was based on a Mach number effect, which produced a different response in the instruments four sensors. The PLS instrument only provided E/Q measurements and could not uniquely identify the ion composition.

In order to simulate the pickup process they used an exosphere model (Hartle et al., 1971, 1973a,b) composed of H and N_2, the constituents known to exist in the exosphere at the time. Because of the finite gyroradii the use of MHD codes to model the interaction does not apply, therefore a multifluid 2D MHD model was developed later by Cravens et al. (1998) to describe the interaction. This effort was then followed by the 3D MHD models of Titan interaction with Saturn's magnetosphere by Ledvina and Cravens (1998) and Kabin et al. (1999). Luhmann (1996) studied the gyromotion of pickup ions around Titan treating them as test particles using a simple 2D lunar wake structure. Ledvina et al. (2000) examined ion trajectories in the vicinity of Titan, treating them as test particles similar to that by Luhmann (1996), but using more realistic electric and magnetic fields from 3-D MHD models of the Titan interaction. These efforts were then followed by that of Brecht et al. (2000) who developed a 3D hybrid calculation of the interaction, which did include the finite gyroradius aspects of the interaction. Their model only included a single ion component, an "ad hoc" ion profile and the cell size was sufficiently large that it could not resolve the "ionopause" boundary (Here we use quotes since this boundary could also be interpreted as being a stagnation boundary, see later discussions.). Their hybrid simulations self-consistently included the pickup ions, where they simulated self-consistent electric and magnetic fields. Nagy et al. (2001) developed a multi-species 3-D MHD model of the interaction between Saturn's magnetosphere and Titan's ionosphere.

For this paper we revisit the analysis of Paper I and provide new insights about the nature of the interaction. In addition to H and N_2, we have added H_2, CH_4 and exothermic nitrogen atoms, N*, to our exospheric model. We then use this model to compute mass loading of the plasma by pickup ions, which are formed primarily by photoionization, electron impact ionization and charge-exchange of the neutral exosphere.

2.0 Voyager 1 Encounter with Titan Revisited

2.1 Encounter Geometry and Inferred Model of Interaction

As shown in Figure 1, the Voyager 1 encounter with Titan occurred when Titan was within Saturn's magnetosphere. It was also near local noon and thus near Saturn's magnetopause. The inset shows the encounter geometry with respect to the nominal co-rotational wake. In Figure 2 we show the Voyager 1 flyby geometry, along with the view axes of the A, B, C and D cups of the plasma instrument during the encounter period. Paper I located the points numbered 1 to 8 along the spacecraft trajectory, where the PLS ion spectra were analyzed to characterize Titan's interaction with Saturn's magnetosphere. The sensor alignment is such that the D cup is pointing approximately into the corotation direction, the C cup has partial alignment along the corotation direction, while the A and B cups look at right angles to the corotation direction. The D cup has a conical field-of-view (FOV) with half-width ~ 45°, while that for the A, B and C cups their FOVs are more complex with considerably larger angular half-width ~ 70° (see Barnett and Olbert, 1986 for a description of the instrument response). During the Voyager 1 flyby, the ambient plasma was moving about 20 degrees from the corotation direction, toward Saturn at a mean speed of 120 km/s (velocity range of 80-150 km s^{-1}, Paper I). The maximum flux of the pickup ions comes from this flow direction and gives the largest signal in the D cup.

Some of the inferred properties of Titan's interaction with Saturn's magnetosphere, as envisioned in Paper I, are shown in Figure 2, where the estimated location of the "ionopause", R_{ion} ~ 4400 km and the exobase, R_{exo} ~ 4000 km are indicated. The Cassini spacecraft, for its planned 40 plus Titan encounters, will come as close as 1000 km or less of Titan's surface. The figure also shows a deflection of the wake by about 20° from the corotational direction, which was interpreted in Paper I to be caused by an inward deflection of the magnetopause due to an increase in solar wind pressure and Titan's close proximity to the magnetopause. The figure shows the cycloidal trajectory of pickup hydrogen ions observed during the spacecraft's inbound leg of Titan's flyby.

2.2 Analysis of Plasma Data: New Results

In Figure 3 we show, as done in Paper I, six of the eight PLS ion spectra analyzed for study of the Titan interaction (spectra 5 and 6 in the ionotail are not included for brevity). Here we note that for this paper we have used the original analysis results of Paper I with regard to modeled simulations of the ion spectra in Figure 3. But for this paper we have modified our original interpretations of the simulations performed in Paper I. Spectra 1 and 8 were measured when the spacecraft was far from the interaction region and showed the presence of very hot ambient magnetospheric plasma. In Paper I we summed the ion spectra far from Titan to get a large scale picture of the ambient ion properties (see Figure 7 in Paper I). As stated previously we modeled in Paper I the ambient ions with convected Maxwellians with a low energy component identified to be H^+ (i.e., confined below a few hundred eV) and a hot keV heavy ion component such as N^+/O^+. The

ambient ions because of their high temperatures are characteristically broad in E/Q space and appear in all four sensors.

In Table 2, we show estimated ion gyro-radii for the ambient plasma, spectrum 1, and possible pickup ion components for spectra 2, 3 and 4. For the ion spectra, the pickup ions modeled as ring distributions will show an increase in amplitude with increasing E/Q until the ion speed is $v_i \sim 2V$ (i.e., V is the local flow speed of the plasma) above which the ion flux will drop precipitously with increasing E/Q (see the paper by Sittler et al., 2004b for an in-depth description of the observational properties of a ring distribution in the spacecraft frame of reference). The presence of pickup ions is clearly seen in the D cup for Figure 3 spectra 2 and 3. The table shows gyro-radii for ambient protons of ~ 400 km, while that for N^+/O^+ of ~ 5600 km, the latter being greater than the diameter of Titan. In our future discussions the guiding center concept will play a critical role in our conclusions. It should also be noted that the positive ions will gyrate in the counter-clockwise direction when looking down upon Figure 2.

Consider, Figure 2 and spectrum 2 in Figure 3. When the spacecraft is ~ 5500 km from the center of the deflected wake, attenuation of ambient heavy ions (N^+/O^+), residing toward keV energies, is apparent. The ambient protons at lower energies are essentially unaffected. Also, there is the possible presence of pickup ions in the D cup at energies extending up to 500-1000 eV. In spectrum 3 the ambient heavy ions are essentially removed and the ambient protons are also showing attenuation toward higher energies. The dominant feature for this spectrum is the presence of a pickup ion component with energy below a few hundred eV. The magnetometer data indicates that spectrum 4 is just outside the wake region. In spectrum 7, when the spacecraft exits the wake, only ambient protons appear and in spectrum 8 both ambient protons and heavy ions have completely recovered. Overall inspection of these figures indicates a preference for the ambient heavy (N^+/O^+) ions to be removed during the inbound pass relative to that on the outbound pass consistent with a finite gyroradius effect.

Continuing this reasoning, we note that the distance Voyager 1 is from the wake region when taking spectrum 2 is of the order of the gyroradii of the ambient heavy ions (N^+/O^+). Thus, upstream heavy ions (N^+/O^+), whose guiding center trajectories pass between the spacecraft and the wake, will have a high probability of gyrating into Titan's atmosphere and be lost from the plasma flow as suggested in spectrum 2. It is important to note that if the ion velocity vector is to point directly into the D cup, the guiding center of the ambient ion must be on the Titan side of the spacecraft position for spectrum 2. Since the D cup has a fairly wide FOV, not all ion trajectories entering the D cup will be attenuated by Titan's extended atmosphere. On the other hand, the ambient protons, having gyroradii of only about 400 km, will not encounter Titan's atmosphere and thus show little attenuation at spectrum 2. Spectrum 3 is only about 1000-2000 km from the wake boundary. Consequently, if ambient heavy ions (N^+/O^+) are to be observed in any of the Faraday cups, their guiding center trajectories must be inside the wake. When this is the case, the ambient N^+/O^+ have a high likelihood of encountering Titan's upper atmosphere and disappear from the plasma flow, as observed. The same can be said for spectrum 7 during the outbound pass. The absence of ambient N^+/O^+ in spectrum 7 is

consistent with their large gyroradii and closeness of the spacecraft to the wake. While the ambient protons with their smaller gyroradii show nearly full recovery. In order for the ions to be observed by cups C and D, their guiding centers must be further away from Titan with respect to the spacecraft and thus increase their probability of not encountering Titan's upper atmosphere. By spectrum 8, the spacecraft is ~ 3000 km from the wake. Since the guiding centers of these ions are on the Saturn side of the spacecraft, they do not encounter Titan's atmosphere and as observed have no attenuation.

As can be inferred from Figure 2, ions entering cups A and B, can have their guiding centers further away from Titan during the inbound pass, relative to that required for cups C and D. There is evidence, especially for cup A, which looks furthest from the corotation direction than the other three sensors, that ambient N^+/O^+ ions are present in spectrum 2 as expected. Cup D in Figure 2 does show some signal up to 5 keV (weaker at lower energies than spectrum 1), but this could be due to a heavy pickup ion component forming further upstream before mass loading has taken effect (i.e., $r_g \sim 7300$ km). Ions observed in spectrum 7 by A and B cups must have their guiding centers shifted toward Titan with respect to ion trajectories sensed by cups C and D. Therefore, the guiding centers of ambient protons must be no closer than ~ 400 km from the upper atmosphere of Titan (i.e., above the exobase). The location of the inferred boundary of the wake, as shown in Figure 2, is consistent with this interpretation. Altogether, it should be clear from the above discussion, that finite gyroradius effects do play an important role in the physics of Titan's interaction with Saturn's magnetosphere. A similar effect as described above was suggested by the hybrid calculations of Brecht et al. (2000), which showed a preference for the ambient ions on one side of the tail and the pickup ions on the other. The finite gyro-radius effects reported here, also clearly show that the hot keV ion component of the ambient plasma is a heavy ion such as N^+/O^+.

Returning to spectrum 2, the location of the high energy edge of the pickup ion peak will be equivalent to twice the flow speed of the plasma if the ions are described by a ring distribution (see previous discussions about ring distributions). In Table 2 we indicate our estimated drift speeds of the plasma for an assumed composition of the pickup ions. If protons, the inferred drift speed of 175 km/s exceeds our upper estimate of 150 km/s for the flow speed of the ambient plasma. In the case of N^+ (equivalent to CH_4^+) the drift speed is ~ 50 km/s, which is below our lower range of 80 km/s for the flow speed of the ambient plasma. But it would be consistent with some mass loading of the plasma by the pickup ions. If the ion is N_2^+, the drift speed is ~ 33 km/s. Note that the gyroradii of the pickup ions are $350 \text{ km} < r_g < 1800$ km, considerably less than the gyroradii of ambient N^+/O^+ ions $r_g \sim 5600$ km. We also note that there is evidence of lower energy pickup ion component in Figure 3, which could be pickup H_2^+ if the higher energy peak is due to pickup N^+ (CH_4^+).

For spectrum 3, where the pickup ions are confined below a few hundred eV, the estimated drift speeds are ~ 85 km/s, 23 km/s and 16 km/s for H^+, N^+ (CH_4^+) and N_2^+, respectively. At this point, considerable mass loading of the plasma has occurred. We also see a further decrease in the gyroradii of the pickup ions, where $170 \text{ km} < r_g < 900$

km. Finally, in spectrum 4, the spectral peak is confined below the low energy cut-off of the PLS instrument, 10 eV, and the inferred flow speeds are 60 km/s, 10 km/s and 5 km/s for H^+, N^+ (CH_4^+) and N_2^+, respectively. Here, the plasma flow is very close to the wake boundary and severe mass loading of the plasma has occurred and is probably composed of N_2^+ ions. At this point, the flow is more fluid like, and the gyroradii are 120 km < r_g < 280 km. In conclusion, we can say, further from the wake, finite gyro-radii effects are dominant, while near the "ionopause" boundary, the flow becomes more fluid like. Therefore, future models must consider these issues. The numerous close encounters of the Cassini spacecraft with Titan will allow us to constrain models of the interaction over a wide range of encounters and Titan interaction geometries, which could include Titan's interactions within Saturn's magnetosheath or the solar wind.

3.0 Titan's Exosphere

3.1 General Exosphere Properties

We extend the exosphere model in Paper I, which included H and N_2, constituents observed at the time. Atmosphere models by Keller et al. (1998), Yung (1987), Yung et al. (1984) and Toublanc et al. (1995) predicted significant quantities of H_2 and CH_4 in the exosphere. We include these species and added the ejection of suprathermal nitrogen atoms, due to electron and photon dissociation of N_2 (Strobel and Shemansky, 1982; Ip, 1992; Strobel et al. 1992) and sputtering due magnetospheric ion impact (Shemantovich 1998, 1999; Shemantovich et al. 2001; Michael et al., 2004). For the suprathermal nitrogen component we use a source strength $S_N \sim 4.5 \times 10^{25}$ atoms/s, which is the value used in Sittler et al. (2004a). The results are shown in Figure 4 for a spherically symmetric model of the exosphere. As can be seen H_2, H and N* dominate far from Titan with H_2 an order of magnitude larger than H, while H is two orders of magnitude larger than N*. Because methane is lighter than N_2 it will dominate for heights greater than a few hundred kilometers above the exobase at r ~ 4000 km, until a height ~ 1500 km when H_2 starts to dominate. Note that the mass density of CH_4 will dominate over that of H_2 for heights up to 2500 km. This will be important when considering mass loading calculations. Finally, when within a few scale heights of the exobase, N_2 will dominate over everything else, especially its mass density. The neutral exospheric densities in Cravens et al. (1998) for radii > 10,000 km are larger than our's by an order of magnitude. They use an estimate of the loss rate $S_N \sim 5 \times 10^{26}$ atoms/s (Barbosa (1987)). At lower heights, where methane dominates, we are in agreement.

4.0 **Mass Loading Calculations: Ionopause Location?**

Using the exosphere model described above, we compute the effects of mass loading on the flow of the ambient plasma due to pickup ions as in Paper I. The "ionopause" altitude is estimated to be the point above the ionosphere where the mass loaded plasma velocity vanishes. The pickup ions are formed by ionizing the neutral exosphere constituents, which include H_2, N*, and CH_4 in addition to H and N_2 used in Paper I. We include photoionization, electron impact ionization and charge exchange reactions in our model calculations. The cross-sections and reaction rates are summarized in Table 3. The

plasma velocity, V, along a streamline, s, is obtained by solving the mass conservation and momentum equations

$$\frac{\partial \rho V}{\partial s} = \sum_j m_j P_j - \sum_k m_k L_k \quad (1a) \qquad \rho V \frac{\partial V}{\partial s} = -2V \sum_j m_j P_j \quad (1b)$$

where,

$$\rho = \sum_j m_j N_j \quad (2a) \qquad V = \sum_j m_j N_j V_j / \sum_j m_j N_j \quad (2b)$$

The total mass density, ρ, and the bulk velocity component, V, along the streamline s are obtained by summing over all ion species whose components include the j-th ion mass, m_j, ion density N_j, and ion velocity, V_j,. P_j is the total volume production rate for the j-th ion and L_k is the charge-exchange volume loss rate of the kth ion. The momentum equation (1b) has been simplified by only including the impulse force due ion pickup, while ignoring the pressure gradient force, $\partial p/\partial s$, and the magnetic force, **j**x**B**. These calculations, which only include mass loading effects and are intrinsically 1D in character, tend to over-estimate the "ionopause" height, while the missing horizontal flow component will move the "ionopause" position inward. Based on the Venus results of Hartle et al. (1980), this boundary would move outward because of the expected pile up of plasma and magnetic field above the "ionopause". This can cause the total pressure gradient force (particle plus field) to point upstream in the same direction as the impulse force. The Cravens et al. (1998) MHD results would argue that the total plasma pressure would be almost a constant above the boundary and have little effect on our predicted "ionopause" location. The numerous Cassini encounters with Titan is expected to identify the differences between Venus and Titan.

In Figure 5, the geometry used for our calculations is shown for a fluid element moving past Titan with impact parameter b. The distance s is the distance traveled by a fluid element through Titan's exosphere and as pickup ions are added to the fluid element it slows due to the impulse term in Eq. 1b. In these calculations we ignore deflections and compressions/expansions of the fluid element as it moves past Titan and are thus 1D in character. The observation point is for a particular spacecraft position, but is more symbolic of an observation point for a continuum of s values. In the case of zero impact parameter, b=0, the fluid element moves towards Titan along the axis parallel to the flow, through the origin, at 20° to the x-axis. When mass loading becomes large, the plasma stops at a boundary we identify as the "ionopause". In Figure 6 we show the reduction in flow speed along a streamline with impact parameter b = 0, where considerable deceleration occurs between 5000 km and 6000 km. Due to the addition of methane we find a slightly larger "ionopause" (~ 4800 km) than was estimated in Paper I (~ 4400 km). We note that the "ionopause" altitude estimated in paper I was where the ion-neutral mean free path equaled the horizontal scale height. Below such an altitude, the ions formed would tend to be tied to the neutral atmosphere and behave more like "ionospheric" ions. One could argue that this boundary is more like a stagnation boundary, since the definition of an ionopause, originally defined for Venus, is where the ionospheric plasma drops off rapidly. In the case of Venus it is where the ionospheric

plasma pressure balances the solar wind pressure. But, as discussed in Sittler and Hartle (1996) for Triton where analogies were made with Venus, the ionopause can be very thick if the external pressure is higher than average and the magnetic field penetrates deeper into the ionosphere. We would argue from the MHD calculations by Cravens et al. (1998) that the ionopause layer will be thick in the case of Titan and that our usage of ionopause boundary is appropriate. But. for now, we will use quotes around the word "ionopause" to indicate potential uncertainty in using this terminology.

We have compared our flow velocity calculations with that by Cravens et al. (1998) for which their ram case is similar to our b=0 case. Their calculations show a more gradual drop in flow speed with decreasing radius over larger scales lengths ~ 10,000 km. This is due to a combination of a) a denser population of suprathermal nitrogen atoms far from Titan (see section 3.1) and b) their use of only photoionization. From looking at Table 3 it is clear that electron impact ionization dominates over photoionization for electron temperatures T_e ~ 200 eV. In their Figure 3 the electron temperature within the magnetosphereic flow is only 5000°K (i.e., ~ 0.5 eV), for which the electron impact ionization rates will be negligible. Their magnetospheric electron temperatures are a factor of 400 below that observed by the Voyager 1 plasma instrument (Hartle et al., 1982). Also, Cravens et al. (1998) used an upstream flow speed of V ~ 95 km/s and not the 120 km/s we have used. Nagy et al. (2001) used the same ion production radial profile as used by Cravens et al. (1998), but a higher upstream flow speed V ~ 120 km/s as used in this paper. As expected, in the Nagy et al. (2001) paper, the slowing down of the flow in the ram direction is similar to that reported by Cravens et al. (1998). They also used the same electron temperature profile as that used by Cravens et al. (1998). These models are inconsistent with the observations of magnetospheric electron temperatures by a significant amount.

At an impact parameter of b = 6000 km, the flow speed decreases considerably before it asymptotes to ~ 60 km/s as the plasma moves past Titan. This speed is lower than expected for H^+ in Table 1. Considering the flow to be 20 degrees or more from the x-axes, as shown in Figure 2, and using the values in Table 1, we would argue that this calculation pertains to spectrum 2, where the pickup ion might be CH_4^+. We note that the gyroradius of CH_4^+ at its birthplace upstream is greater than the scale height of its source unlike for H and H_2. In this case, the observed cutoff energy is expected to be less than that corresponding to 2 times the drift speed of the ambient plasma (Hartle and Sittler, 2004). Therefore, the pickup ion will not have reached its maximum velocity at the observation site. Consequently, the 47 km/s at for CH_4^+ in Table 1 is a lower limit. In the case of b = 5558 km, the flow speed decreases to an asymptotic value ~ 5 km/s as the fluid element moves past Titan. This case is consistent with spectrum 4 when the "ionopause" is ~ 4800 km. Table 2 shows the drift speed to be ~ 5 km/s for pickup N_2^+. For lower impact parameters the flow decreases rapidly. Under these circumstances, the flow must be moving tangent to the "ionopause" boundary. Spectrum 3 would be intermediate to cases b = 6000 km and 5558 km.

Our calculations have ignored the effects of the plasma pressure gradient force and the magnetic force, which may tend to cancel each other out. Since the above calculation

using (Eqs. 1 a, b) is a fluid approximation, the impulse force assumes that the ions are instantaneously picked up at the ambient drift speed. This tends to overestimate the impulse force due to finite gyroradius. The problem arises because heavy ions like N_2^+ have gyroradii that are much larger than the scale height of the source gas. Such ions born in the last scale height or two above the ionopause may never attain the ambient drift speed over the acceleration region studied, thereby leading to an overestimate of the impulse force. Consequently, finite gyroradius corrections would put the "ionopause" below 4800 km. However, the altitude where ion neutral drag stops the flow would determine the ultimate limit.

5.0 **Summary and Conclusion**

We have presented a new analysis of the plasma observations by Hartle et al. (1982) (Paper I). Initial results were presented in the paper by Sittler et al. (2004c) for the conference on Titan at ESTEC in April 13-17, 2004. Here we emphasize the importance of finite gyroradius effects in the analysis of Voyager 1 plasma data, which show an asymmetric removal of ambient ions from the plasma flow by Titan's extended atmosphere. As indicated by the viewing geometry of the plasma instruments's four sensors, and the spacecraft's position along its track past Titan, the ambient ions were preferentially lost on the side of the tail where pickup ions were observed. This was consistent with the viewing geometry of the plasma instrument's four sensors and the spacecraft position along its track past Titan. For the D cup to see ambient ions for spectrum 2, the ion guiding centers had to be offset toward Titan relative to the spacecraft and thus had a greater probability of encountering Titan's upper atmosphere, while on the outbound pass the reverse was true. This feature of the data is consistent with the 3D hybrid calculations by Brecht et al. (2000). Here we emphasize that when looking down on Figure 2 the ions are gyrating in the counter-clockwise direction. Including the finite gyro-effects, reinforce the analysis in Paper I that the ambient ions were composed of a light (H^+) and heavy ion component (N^+/O^+).

We have upgraded the exosphere model in Paper I to include H_2, CH_4 and N^*, in addition to the H and N_2 used in Paper I. Using this revised exosphere model we have calculated the effects of mass-loading on the external flow using a simple 1D model. But, mass loading alone cannot determine the "ionopause" location, since the upstream flow can dominate the mass loading term. Ignoring this caveat, we then compared our mass loading calculations with the plasma ion spectra and showed that the pickup ions in spectrum 2 were consistent with CH_4^+ ions. However, there may also have been some evidence of heavy ions being picked up somewhere upstream and then observed by the plasma instrument at energies ~ 5 keV (i.e., ion gyroradii ~ 7800 km). We then showed that spectrum 3 was probably CH_4^+, although N_2^+ could not be ruled out. Finally, spectrum 4 was very likely N_2^+. This is a revision of the original analysis in Paper I, where it was proposed that H^+ was the likely pickup ion for spectra 2 and 3. This was before the authors were aware of the likely presence of CH_4 in Titan's exosphere (Keller et al., 1998; Yung, 1987; Yung et al., 1984; Toublanc et al., 1995). Here we show that H_2^+ pickup ions will dominate at larger altitudes, followed by CH_4^+ pickup ions and then at altitudes just above the "ionopause" N_2^+ pickup ions will dominate the mass loading.

In our calculations we ignored the effects of the upstream plasma pressure, magnetic field pressure and magnetic tension, all of which will tend to move the "ionopause" to lower altitudes. For impact parameter b = 0, we estimate the mass loading force to be $F_{ML} \sim 4.5x10^{-11}$ dyne/cm^2 at the nose of the "ionopause", while the upstream magnetic field pressure will be $F_M = B^2/8\pi \sim 10^{-10}$ dyne/cm^2 for a field strength B ~ 5 nT. The upstream plasma pressure $p \sim 10^{-9}$ dyne/cm^2, with plasma $\beta \sim 11$ as reported by Neubauer et al. (1984). Therefore, $p >> F_M > F_{ML}$ so that mass loading alone will probably not define the actual position of the "ionopause" or its thickness. The model calculations by Galand et al. (1999) give an "ionopause" density of $N_e \sim 2000$ electrons/cm^3 at an altitude z ~ 1000 km or r ~ 3600 km. If we impose pressure balance at the "ionopause" then

$$P = p + F_M = N_e k_B (T_i + T_e)$$

$P \sim 10^{-9}$ dyne/cm^2 is the upstream plasma pressure and magnetic field pressure. Ignoring a possible magnetic field in the ionosphere, we can get pressure balance altitude of z ~ 1000 km if we set $T = (T_i + T_e)/2 \sim 1800$ K which is much greater than the neutral gas temperature of T ~ 180 K of the upper atmosphere, as originally derived from the Voyager 1 observations by Broadfoot et al. (1981). If there is significant penetration of the magnetic field into the ionosphere then this temperature estimate for the ionosphere will be reduced. Therefore, the "ionopause" location resides somewhere between 3600 km < R_{ion} < 4800 km. This feature of the interaction is similar to that calculated by Cravens et al. (1998). They found a similar location and thickness of this "ionopause" layer estimated here, 3600 km < r < 4800 km, and confirm the general validity of our calculations. But, as previously emphasized, the ability to properly characterize this boundary one must use a hybrid code similar to that developed by Brecht et al. (2000) at high altitudes, which then transitions to an MHD calculation at lower altitudes where the flow is more fluid like.

The above analysis suggests that there is still much to learn from data expected from the multiple passes through Titan's upper atmosphere by Cassini. For instance, the above argument ignores the fact that the slowing down by mass loading is usually accompanied by piling up of magnetic field and plasma (ambient and new born ions). The piled up field and plasma can add significantly to pressure and pressure gradient forces as discussed in Hartle et al. (1980) for Venus. In addition, we note that although $F_{ML} << P$, the scale length for F_{ML} at the boundary where mass loading is most important (i.e., r ~ 4800 km and b = 0) is $L_{ML} \sim 100$ km, while for P it is L ~ 1000 km. Therefore, at this boundary mass loading can dominate over pressure gradients and there could be a sudden drop in flow speed at this boundary. Inside this boundary inward motion of the plasma to the ionosphere would be dominated by pressure gradients in the plasma. These estimates also indicate that there could be considerable mixing of the magnetospheric plasma with Titan's upper atmosphere for 3600 km < r < 4800 km (Brecht et al., 2000). These features of the interaction are similar to that calculated by Cravens et al. (1998), who used a 2D MHD code. One also expects the thickness of the "ionopause" to be ~ an ion gyroradius, which for Titan could be several hundred kilometers thick or more as suggested by our previous arguments.

The location of the "ionopause" is critical in determining whether the pickup ions efficiently interact with the region below the exobase causing atmospheric loss (Shematovich et al., 2001; Michael et al., 2004) and whether magnetospheric electrons have access to the atmosphere below the exobase (see Strobel and Shemansky, 1982). Strobel et al. (1992) used arguments similar to those in Paper I to put the "ionopause" at $R_{ion} \sim 4400$ km. If true, their result would prevent the magnetospheric plasma from having access to Titan's upper atmosphere and thus downgrade the importance of the exothermically produced nitrogen atoms with regard to the nitrogen torus surrounding Saturn. They estimated that the source strength for the escaping N atoms would be reduced from $S_N \sim 3x10^{26}$ atoms/s as originally proposed by Strobel and Shemansky (1982) to be $S_N \sim 10^{25}$ atoms/s. If the "ionopause" is rather at $r < 4400$ km, then the source term for exothermically produced nitrogen could be considerably greater. Ip (1992) and Sittler et al. (2004a) discuss these issues in more detail.

Because the upstream plasma and magnetic field can have pressures large compared to ionospheric pressures without heating, the ionosphere could be highly compressed with a correspondingly thick "ionopause" residing between 3600 km and 4800 km. Sittler and Hartle (1996) discussed a similar situation for Triton, where they made analogies with Venus' ionosphere. Under these circumstances energetic electrons will tend to gradient drift around Titan and not have direct access to its upper atmosphere for altitudes less than 1000 km. This could have an important effect on models of Titan's ionosphere, such as that by Galand et al. (1999).

REFERENCES

1. Albritton, D. L., Ion-neutral reaction-rate constants measured in flow reactors through 1977, *At. Nucl. Data Tables, 22*, 1-101, 1978.
2. Barnett, A. and S. Olbert, Response function of modulated grid Faraday cup plasma instruments, *Rev. Sci. Instrum.*, **57**, 2432, 1986.
3. Basu et al., Linear transport theory of auroral proton precipitation: A comparison with observations, *J. Geophys. Res.*, **92**, 5920-5932, 1987.
4. Brecht, S. H., Luhmann J. G. and Larson D. J., Simulation of the Saturnian magnetospheric interaction with Titan, *J. Geophys. Res.*, **105**, 13,119-13,130, 2000.
5. Bridge, H.S., J.W. Belcher, R.J. Butler, A.J. Lazarus, A.M. Mavretic, J.D. Sullivan, G.L. Siscoe and V.M. Vasyliunas, The plasma experiemtn on the 1977 Voyager Mission, *Space Sci. Rev.,* **21**, 259, 1977.
6. Bridge, H. S., et al., Plasma observations near Saturn: Initial results from Voyager 1, *Science*, **212**, 217, 1981.

7. Cravens, T. E., C. J. Lindgren and S. A. Ledvina, A two-dimensional multi-fluid MHD model of Titan's plasma environment, *Planet. Space Sci.*, **46**, 1193-1205, 1998.
8. Freysinger, W. et al., "Charge-transfer reaction of $^{14,15}N^{+}(^{3}P_{J})+N_{2}(^{1}\Sigma_{g}^{+})$ from thermal to 100 eV Crossed-beam and scattering-cell guided-ion beam experiments", J. Chem. Phys. 101, 3688-3695, 1994.
9. Galand, M., J. Lilensten, D. Toublanc and S. Maurice, The ionosphere of Titan: Ideal diurnal and nocturnal cases, *Icarus*, **140**, 92, 1999.
10. Hartle, R. E., Model for rotating and non-uniform planetary exospheres, *The Physics of Fluids*, **14**, 2592, 1971.
11. Hartle, R. E., Density and temperature distributions in non-uniform rotating planetary exospheres with application to Earth, *Planet. Space Sci.*, **21**, 2123, 1973.
12. Hartle, R. E., K. W. Ogilvie and C. S. Wu, Neutral and ion-exospheres in the solar wind with application to Mercury, *Planet. Space Sci.*, **21**, 2181, 1973.
13. Hartle, R. E., H. A. Taylor, Jr., S. J. Bauer, L. H. Brace, C. T. Russel and R. E. Daniell, J.r, Dynamical response of the dayside ionosphere of Venus to the solar wind, *J. Geophys. Res.,* **85**, 1980.
14. Hartle, R. E., E.C. Sittler Jr., K. W. Ogilvie, J. D. Scudder, A.J. Lazarus and S. K. Atreya, Titan's ion exosphere observed from Voyager 1, *J. Geophys. Res.*, **87**, 1383, 1982.
15. Hartle, R. E. and E. C. Sittler, Jr., Pickup ion velocity distributions at Titan: Effects of spatial gradients, *Eos. Trans.* AGU, **85(17)**, Joint Assembly Suppl., Abstract, P33D-04, 2004.
16. Huebner, W. F. and P. T. Giguere, A model of comet comae,II, Effects of solar photodissociation ionization, *Astrophys. J.*, **238**, 753, 1980.
17. Huntress, W. T., Jr., Laboratory studies of bimolecular reactions of positive ions in interstellar clouds, in comets, and in planetary atmospheres of reducing composition, *Astrophys. J. Suppl. Ser.*, **33**, 495-514, 1977.
18. Ip, W., -H., The nitrogen tori of Titan and Triton, *Adv. Space Res.*, **12**, (8)73, 1992.
19. Kabin, K., T. I. Gombosi, D. L. Zeeuw, K. G. Powell, and P. L. Israelevich, Interaction of the Saturnian magnetosphere with Titan: Results of a three-dimensional MHD simulation, *J. Geophys. Res.*, **104**, 2451, 1999.
20. Keller, C. N., V. G. Anicich and T. E. Cravens, Model of Titan's ionosphere with detailed hydrocarbon ion chemistry, *Planet. Space Sci.*, **46**, 1157-1174, 1998.
21. Koopman, D. W., Charge exchange in CH_4 and NH_3*, *J. Chem. Phys.*, **49**, 5203, 1968.
22. Ledvina, S. and T. E. Cravens, A three-dimensional MHD model of plasma flow around Titan, *Planet. Space Sci.*, **46**, 1175, 1998.
23. Ledvina, S. A., T. E. Cravens, A. Salman and K. Kecskemety, Ion trajectories in Saturn's magnetosphere near Titan, *Adv. Space Res.*, **26**, 1691, 2000.
24. Lo, H. H., et al., Electron capture and loss collisions of heavy ions with atomic oxygen, *Phys. Rev.*, **A4**, 1462-1476, 1971.
25. Lotz, W., Electron-impact ionization cross-sections and ionization rate coefficients for atoms and ions, *Astrophys. J. Suppl. Ser.*, **14**, 207-238, 1967.

26. Luhmann, J. G., Titan's ion exospheric wake: A natural ion mass spectrometer?, *J. Geophys. Res. – Pl.*, **101**, 29387, 1996.
27. Massay, H. S. and H. B. Gilbody, Electronic and ionic impact phenomena, in *Recombination and Fast Collisions of Heavy Particles*, vol. IV, Oxford University Press New York, pp. 2782, 1974.
28. Michael, M., R. E. Johnson, F. Leblanc, M. Liu, J. G. Luhmann, and V. I. Shematovich, "Ejection of Nitrogen from Titan's Atmosphere by Magnetospheric Ions and Pickup Ions", *Icarus*, in press, 2004.
29. Nagy, A. F., Y. Liu, K. C. Hansen, K. Kabin, T. I. Gombosi, M. R. Combi, D. L. DeZeeuw, K. G. Powell and A. J. Kliore, The interaction between the magnetosphere of Saturn and Titan's ionosphere, *J. Geophys. Res.*, **106**, 6151, 2001.
30. Neubauer, F.M., D.A. Gurnett, J.D. Scudder, and R.E. Hartle, Titan's magnetospheric interaction, in *Saturn,* eds. T. Gehrels and M.S. Matthews, Univ. of Arizona Press, Tucson, 571, 1984.
31. Ness, N. F., M. H. Acuna, R. P. Lepping, J. E. P. Connerney, K. W. Behannon, L. F. Burlaga, F. M. Neubauer, Magnetic field studies by Voyager 1: Preliminary results at Saturn, *Science*, **212**, 211, 1981.
32. Ness, N. F., M. H. Acuna, K. W. Behannon, and F. M. Neubauer, The induced magnetosphere of Titan, *J. Geophys. Res.*, **87**, 1369-1381, 1982.
33. Newman, J. H., J. D. Cogan, D. L. Ziegler, D. E. Nitz, R. D. Rundel, K. A. Smith and R. F. Stebbings, Charge transfer in H^+-H and H^+ - D collisions within the energy range 0.1 – 150 eV, *Phys. Rev. A.*, **25**, 2976, 1982.
34. Phaneuf, R.A., et al., Single-electron capture by multiply charge ions of carbon, nitrogen and oxygen in atomic and molecular hydrogen, *Phys. Rev.*, **A4**, 534-545, 1978.
35. Phelps, A. V., Cross sections and swarm coefficients for nitrogen ions and neutrals in N_2 and Argon ions and neutrals in Ar for energies from 0.1 eV to 10 eV, *J. Phys. Chem.Ref. Data*, **20**, 557-573, 1991.
36. Rapp, D. and P. Englander-Golden, Total cross sections for ionization and attachment in gases by electron impact. I. Positive ionization, *J. Chem. Phys.*, **43**, 1464, 1965.
37. Rees, M. H., "Physics and chemistry of the upper atmosphere", Cambridge Univ. Press, 1989.
38. Rudd, M. E., Y.-K., D. H. Madison and J. W. Gallagher, Electron production in proton collisions: total cross sections, *Rev. Mod. Phys., Vol. 57, No. 4,* 965, 1985.
39. Shemantovich, V.I., Kinetic modeling of suprathermal nitrogen atoms in the Titan's atmosphere: I. Sources, *Solar System Research,* **32**, 384, 1998.
40. Shemantovich, V.I., Kinetic modeling of suprathermal nitrogen atoms in the Titan's atmosphere: II. Escape flux due to dissociation processes, *Solar System Research,* **33**, 32, 1999.
41. Shematovich, V.I., C. Tully and R.E. Johnson, Suprathermal nitrogen atoms and molecules in Titan's corona, *Adv. Space Res.,* **27**, 1875-1880, 2001.
42. Sittler, E. C., Jr., K. W. Ogilvie and J. D. Scudder, Survey of low energy plasma electrons in Saturn's magnetosphere: Voyager 1 and 2, *J. Geophys. Res.*, **88**, 8847, 1983.

43. Sittler, E. C., Jr. and R. E. Hartle, Triton's ionospheric source: Electron Precipitation or Photoionization, *J. Geophys. Res.*, **101**, 10,863, 1996.
44. Sittler, E. C., Jr., R.E. Johnson, H.T. Smith, J.D. Richardson, S. Jurac, M. Moore, J.F. Cooper, B. H. Mauk, M. Michael, C. Paranicas, T. P. Armstrong, and B. Tsurutani, Energetic Nitrogen Ions within the Inner Magnetosphere of Saturn, *J. Geophys. Res.*, submitted, 2004a.
45. Sittler, E.C., Jr.,R.E. Johnson, S. Jurac, J.D. Richardson, M. McGrath ,F. Crary, D. Young and J.E. Nordholt, Pickup ions at Dione and Enceladus: Cassini Plasma Spectrometer Simulations, *J. Geophys. Res.,* **109**, A01214, 2004b.
46. Sittler, E. C., Jr., R. E. Hartle, A. F. Vinas, R. E. Johnson, H. T. Smith and I. Mueller-Wodard, Titan interaction with Saturn's magnetosphere: mass loading and ionopause location, *Proceedings of the International Conference TITAN From Discovery to Encounter,* 13-17 April 2004, ESTEC, Noordwijk, The Netherlands, SP-1278, 377, 2004c.
47. Strobel, D.F. and D.E. Shemansky, EUV emission from Titan's upper atmosphere: Voyager 1 encounter, *J. Geophys. Res.*, **87**, 1361-1368, 1982.
48. Strobel, D.F., M.E. Summers and X. Zhu, Titan's upper atmosphere: Structure and ultraviolet emissions, *Icarus,* **100**, 512, 1992.
49. Tawara, H., Cross sections for charge transfer of hydrogen beams in gases and vapors in the energy range 10 eV – 10 keV, *At. Data Nucl. Data Tables,* **22**, 491-525, 1978.
50. Tawara, H. et al, "Cross sections for electron capture and loss by positive ions in collisions with atomic and molecular Hydrogen", Atomic Data and nuclear Data Tables 32, 235-303,1985. .
51. Toublanc, D., J. P. Parisot, D. Gautier, F. Raulin and C. P. McKay, Photochemical modeling of Titan's atmosphere, *Icarus*, **113**, 2, 1995.
52. Yung, Y. L., An update of nitrile photochemistry on Titan, *Icarus*, **72**, 468, 1987.
53. Yung, Y. L., M. Allen and J. P. Pinto, Photochemistry of the atmosphere of Titan: Comparison between model and observations, *Astrophys. J. Suppl.*, **55**, 465, 1984.

Table 1. Plasma Upstream Properties: Voyager 1 Titan Flyby[1]

Parameter	Value
Magnetic Field B	5 nT
Flow Speed V	80-150 km/s
Proton Density n_p	0.1 cm^{-3}
Nitrogen Ion Density n_{N+}	0.2 cm^{-3}
Electron Temperature T_e	200 eV
Proton Temperature T_p	210 eV
N^+ Temperature T_{N+}	2.9 keV
Total Plasma Pressure p	10^{-9} dyne/cm^2
Plasma β	11
Alfven Speed V_A	64 km/s
Sound Speed V_S	210 km/s
Alfven Mach Number $M_A=V/V_A$	1.9
Sonic Mach Number $M_S = V/V_S$	0.57

1. Parameters derived from Hartle et al. (1982) and Neubauer et al. (1984)

Table 2. Ion Drift Speeds and Gyro-Radii at Titan

Spectrum #	Parameter	H^+	N^+	N_2^+
1	Thermal Speed	200 km/s	200 km/s	140.0 km/s
1	Gyro-Radius	400 km	5600 km	7840 km
2	Drift Speed	175 km/s	47 km/s	33 km/s
2	Gyro-Radius	350 km	1316 km	1848 km
3	Drift Speed	85 km/s	23 km/s	16 km/s
3	Gyro-Radius	170 km	636 km	896 km
4	Drift Speed	60 km/s	10 km/s	5 km/s
4	Gyro-Radius	120 km	280 km	280 km

Table 3A. Photoionization Rates

Reaction	Reaction Rate sec^{-1}	Reference
$H_2 + h\nu \rightarrow H^+ + H + e$	10^{-10}	Huebner & Giguere, 1980
$H_2 + h\nu \rightarrow H_2^+ + e$	5.9×10^{-10}	Huebner & Giguere, 1980
$H + h\nu \rightarrow H^+ + e$	8×10^{-10}	Huebner & Giguere, 1980
$N + h\nu \rightarrow N^+ + e$	2×10^{-9}	Huebner & Giguere, 1980
$N_2 + h\nu \rightarrow N_2^+ + e$	3.9×10^{-9}	Huebner & Giguere, 1980
$CH_4 + h\nu \rightarrow CH_4^+ + e$	6.5×10^{-9}	Huebner & Giguere, 1980

Table 3B. Electron Impact Ionization Rates[1]

Reaction	Reaction Rate cm^3/s	Reference
$H + e \rightarrow H^+ + 2e$	5.13×10^{-9}	Lotz, 1966
$H + e^* \rightarrow H^+ + 2e$	3.1×10^{-8}	Lotz, 1966
$H_2 + e \rightarrow H^+ + H + 2e$	6.3×10^{-9}	Rapp & Englander-Golden, 1965

$H_2 + e^* \rightarrow H^+ + H + 2e$	$5.13x10^{-8}$	Rapp & Englander-Golden, 1965
$N_2 + e \rightarrow N_2^+ + 2e$	$1.02x10^{-8}$	Rapp & Englander-Golden, 1965
$N_2 + e^* \rightarrow N_2^+ + 2e$	$1.64x10^{-7}$	Rapp & Englander-Golden, 1965
$CH_4 + e \rightarrow CH_4^+ + 2e$	$2.33x10^{-8}$	Rapp & Englander-Golden, 1965
$CH_4 + e^* \rightarrow CH_4^+ + 2e$	$2.2x10^{-7}$	Rapp & Englander-Golden, 1965
$N + e \rightarrow N^+ + 2e$	$6.59x10^{-9}$	Lotz, 1966
$N + e^* \rightarrow N^+ + 2e$	$9x10^{-8}$	Lotz, 1966

1. We use "e" to represent hot secondaries with $T_e \sim 10$ eV and use "e*" to indicate magnetospheric electrons with $T_e \sim 200$ eV.

Table 3C. Charge Exchange Reaction Rates

Reaction	Reaction Rate cm^3/s (225km/s)	Cross section $10^{-16}cm^2$ (260 eV/amu)	Reference
$H^+ + H \rightarrow H + H^+$	$5.0x10^{-8}$	22.0	Tawara 1985; Newman et al., 1982
$H^+ + H_2 \rightarrow H + H_2^+$	$17.x10^{-10}$	0.77	Tawara 1985; Tawara, 1978
$H_2^+ + H_2 \rightarrow H_2 + H_2^+$	$6.6x10^{-9}$	2.9	Massey & Gilbody, 1974
$H_2^+ + H \rightarrow H_2 + H^+$	$2.25x10^{-8}$	10.0	Estimate
$H^+ + N \rightarrow H + N^+$ [1]	10^{-8}	4.4	Basu et al., 1987
$H^+ + N_2 \rightarrow H + N_2^+$	$2.3x10^{-9}$	1.02	Rees, 1989; Rudd et al., 1985
$H^+ + N_2 \rightarrow H^+ + N_2^+$ [5]	$4.5x10^{-10}$	0.2	Basu et al., 1987
$H^+ + CH_4 \rightarrow H + CH_4^+$	$7x10^{-8}$	31.0	Rudd et al., 1985; Koopman, 1968
$H_2^+ + N \rightarrow H_2 + N^+$	$2.25x10^{-8}$	10.0	Estimate
$H_2^+ + N_2 \rightarrow H_2 + N_2^+$	$4.5x10^{-9}$	2.0	Estimate
$H_2^+ + CH_4 \rightarrow H_2 + CH_4^+$	$4.8x10^{-8}$	21.	Koopman, 1968
$N^+ + CH_4 \rightarrow N + CH_4^+$	$9.4x10^{-10}$	0.42	Albritton, 1978
$N_2^+ + CH_4 \rightarrow N_2 + CH_4^+$ [2]	10^{-9}	0.44	Albritton, 1978
$N^+ + N \rightarrow N + N^+$ [3]	$1.4x10^{-8}$	6.2	Lo et al., 1971
$N^+ + N_2 \rightarrow N + N_2^+$	$1.7x10^{-8}$	7.5	Phelps, 1991
$N^+ + H \rightarrow N + H^+$ [4]	$1.7x10^{-8}$	7.5	Tarawa 1985; Phaneuf et al., 1978
$N^+ + H_2 \rightarrow N + H_2^+$ [4]	$8.4x10^{-9}$	3.7	Tarawa 1985 ; Phaneuf et al., 1978
$N_2^+ + N \rightarrow N_2 + N^+$	10^{-11}	0.0044	Albritton, 1978
$N_2^+ + H \rightarrow N_2 + H^+$	$4.5x10^{-8}$	20	Estimate
$N_2^+ + N_2 \rightarrow N_2 + N_2^+$	$0.7x10^{-8}$	3.	Estimate

$CH_4^+ + H \rightarrow CH_4 + H^+$	$0.4x10^{-8}$	2	Estimate
$CH_4^+ + H_2 \rightarrow CH_4 + H_2^+$	$0.2x10^{-8}$	1.	Estimate
$CH_4^+ + N \rightarrow CH_4 + N^+$	$0.1x10^{-8}$	0.5	estimate
$CH_4^+ + N_2 \rightarrow CH_4 + N_2^+$	$0.1x10^{-8}$	0.5	Estimate
$CH_4^+ + CH_4 \rightarrow CH_5^+ + CH_3$	$1.15x10^{-9}$	0.57	Huntress, 1977

1. Used $H^+ + O \rightarrow H + O^+$ reaction at $E_p = 1$ keV
2. Actual end products are CH_3^+ & CH_2^+
3. Used $N^+ + O \rightarrow N + O^+$ reaction at E = 40 keV
4. Used cross-section at $E_{N+} = 10$ keV
5. Used cross-section at $E_p = 1$ keV

Figure Captions

Figure 1. Figure shows the trajectories of the various spacecraft (Pioneer 11, Voyager 1 and Voyager 2) as they pass through Saturn's magnetosphere. Bow shock (BS) and magnetopause (MP) boundaries are shown (Derived from Figure 1 in Sittler et al. (1983)). It also shows Titan's trajectory around Saturn and its position during the Voyager 1 closest approach with Titan (TCA), one day before TCA and one day after TCA. This figure shows the closeness of Titan to the magnetopause as Voyager 1 made its close encounter with Titan. We then show a blow up of the encounter geometry at TCA (Derived from Hartle et al., 1982). Here, the nominal corotational wake is shown, sunlit side of Titan indicated and the alignment of the plasma instrument's four potential modulated Faraday cups.

Figure 2. Rendition of the interaction of Titan's upper atmosphere with Saturn's magnetosphere as observed by the Voyager 1 spacecraft during its close encounter with Titan as originally proposed by Hartle et al. (1982). The figure shows the alignment of the PLS sensors A, B, C and D relative to Titan and the upstream flow. The figure also shows the spacecraft trajectory and the ion spectra recorded by the plasma instrument and numbered 1 to 8.

Figure 3. This figure shows the ion spectra recorded by the PLS instrument for those outside the wake region. This figure shows the response of the instrument to the ambient plasma, its interaction with Titan and the presence of pickup ions.

Figure 4. Model of Titan's exosphere, which includes H, H_2, N^*, CH_4 and N_2, that was used for our mass loading calculations. See text for details.

Figure 5. Shows geometry of mass loading calculations with fluid element shown as it accumulates pick up ions and are then observed at the spacecraft position which is downstream from the flow. The length of the streamline is indicated by s and the impact parameter b is also shown.

Figure 6. This figure shows the effects of mass loading for various impact parameters of the flow relative to Titan's center. See text for details.

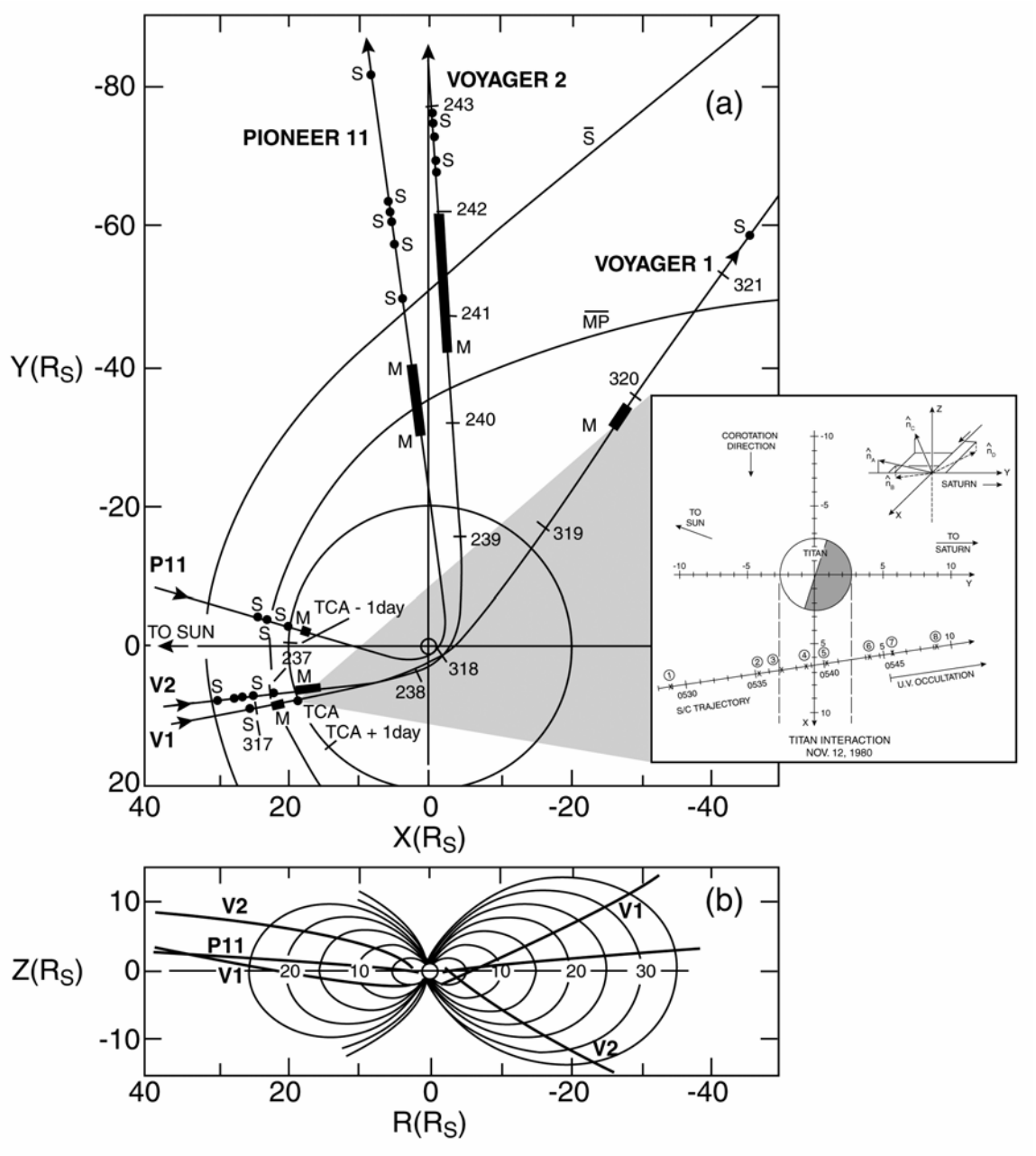
VOYAGER 2
PIONEER 11
VOYAGER 1
(a)
(b)
P11
V2
V1
TO SUN
TCA - 1day
TCA
TCA + 1day
Y(R_S)
X(R_S)
Z(R_S)
R(R_S)
COROTATION DIRECTION
SATURN
TITAN
S/C TRAJECTORY
U.V. OCCULTATION
TITAN INTERACTION
NOV. 12, 1980

Figure 1.

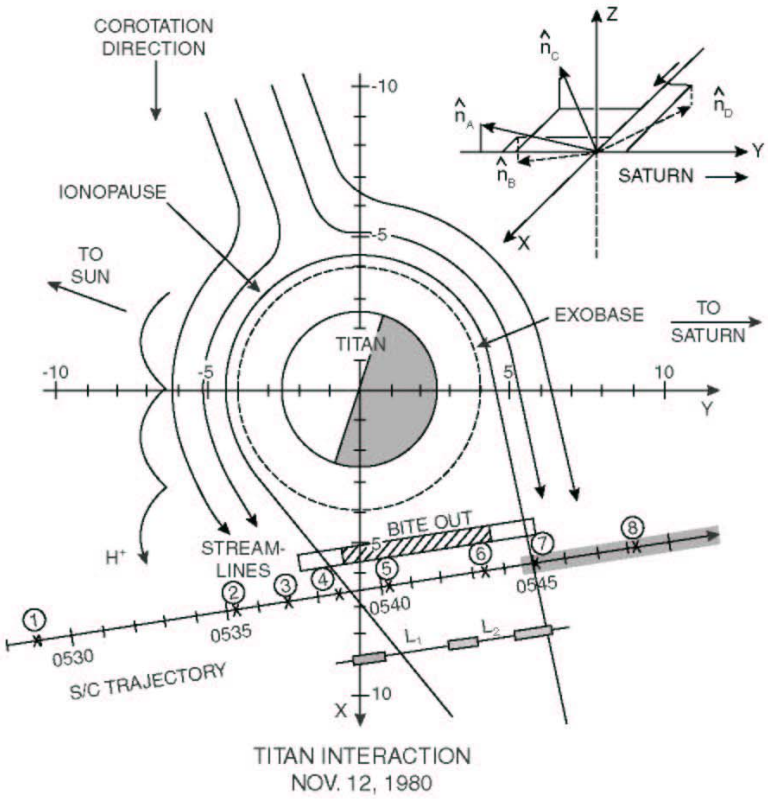
COROTATION
DIRECTION
IONOPAUSE
TO
SUN
TO
SATURN
EXOBASE
TITAN
BITE OUT
STREAM-
LINES
H+
S/C TRAJECTORY
0530
0535
0540
0545
L1
L2
SATURN
Z
Y
X
-10
-5
5
10
TITAN INTERACTION
NOV. 12, 1980

Figure 2.

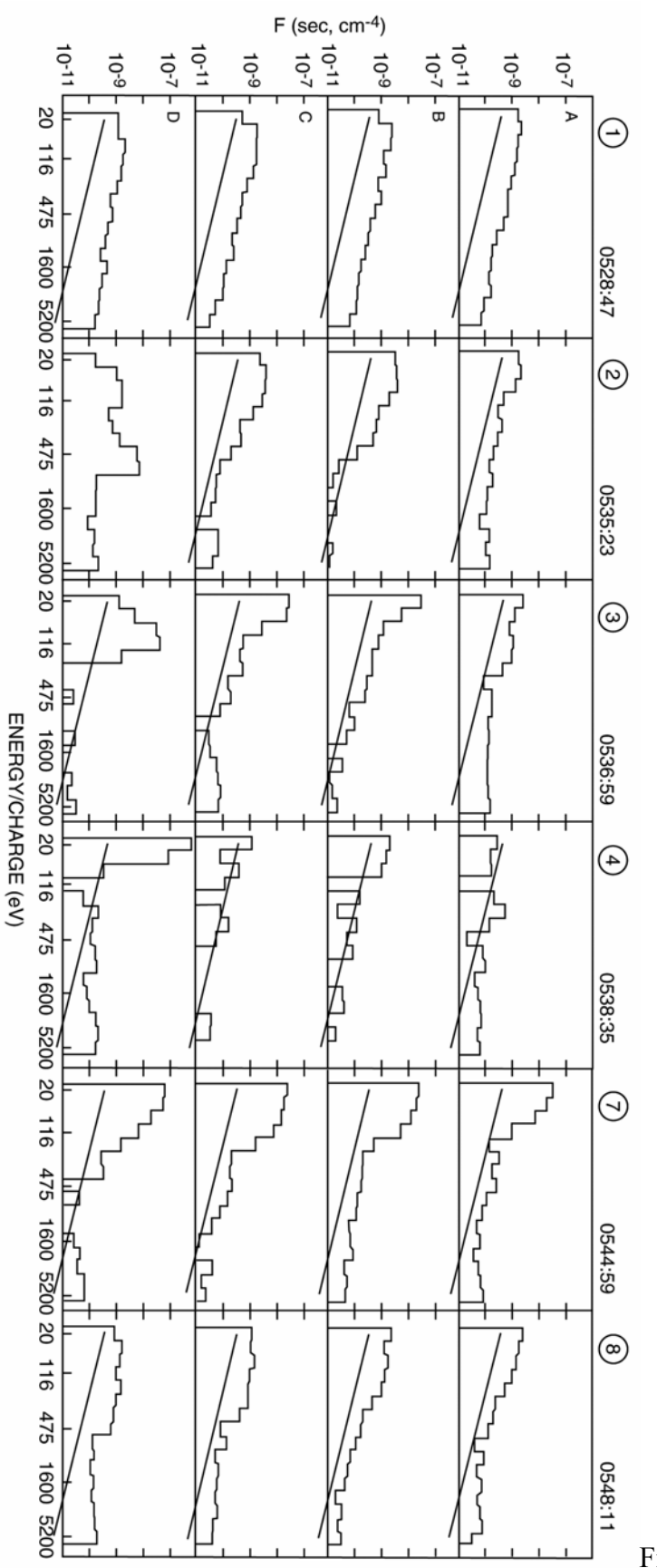
F (sec, cm-4)
A
B
C
D
0528:47
0535:23
0536:59
0538:35
0544:59
0548:11
ENERGY/CHARGE (eV)

Figure 3.

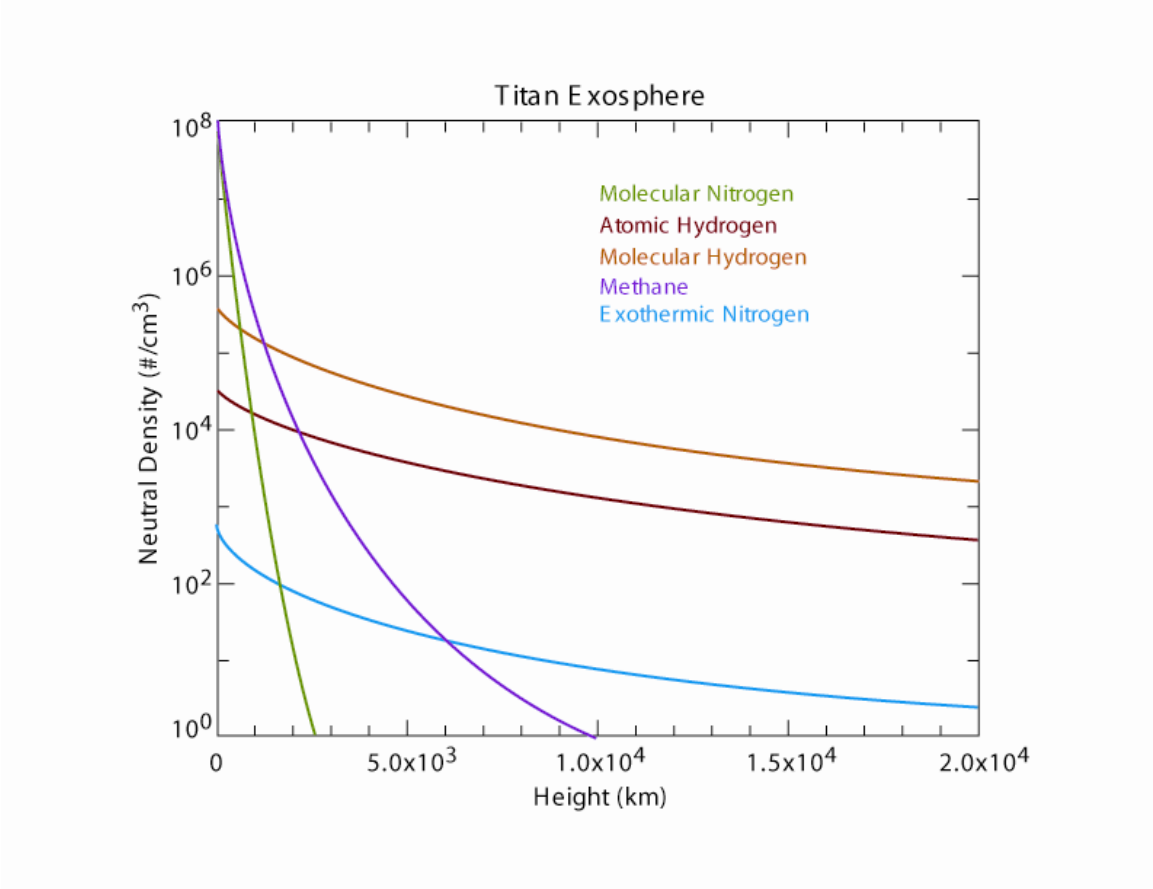
Titan Exosphere
Molecular Nitrogen
Atomic Hydrogen
Molecular Hydrogen
Methane
Exothermic Nitrogen
Neutral Density (#/cm3)
10^8
10^6
10^4
10^2
10^0
0
5.0x10^3
1.0x10^4
1.5x10^4
2.0x10^4
Height (km)

Figure 4

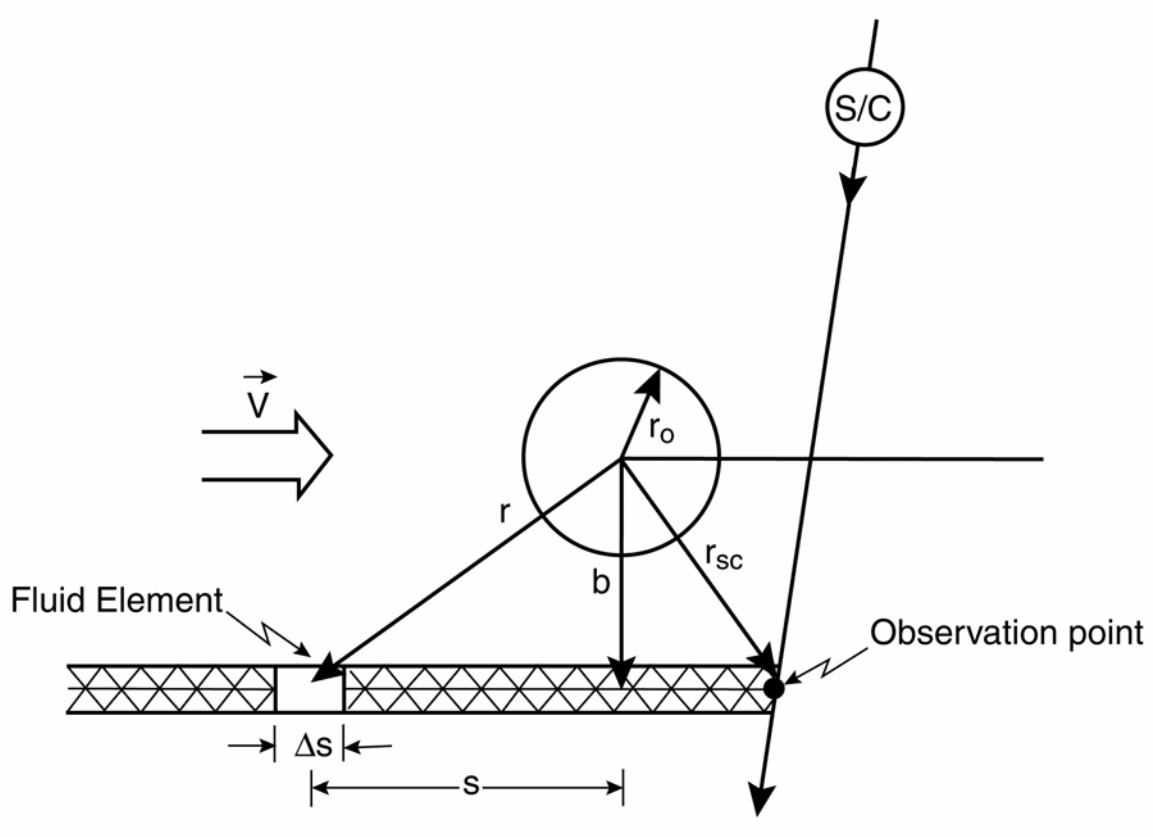

Figure 5.

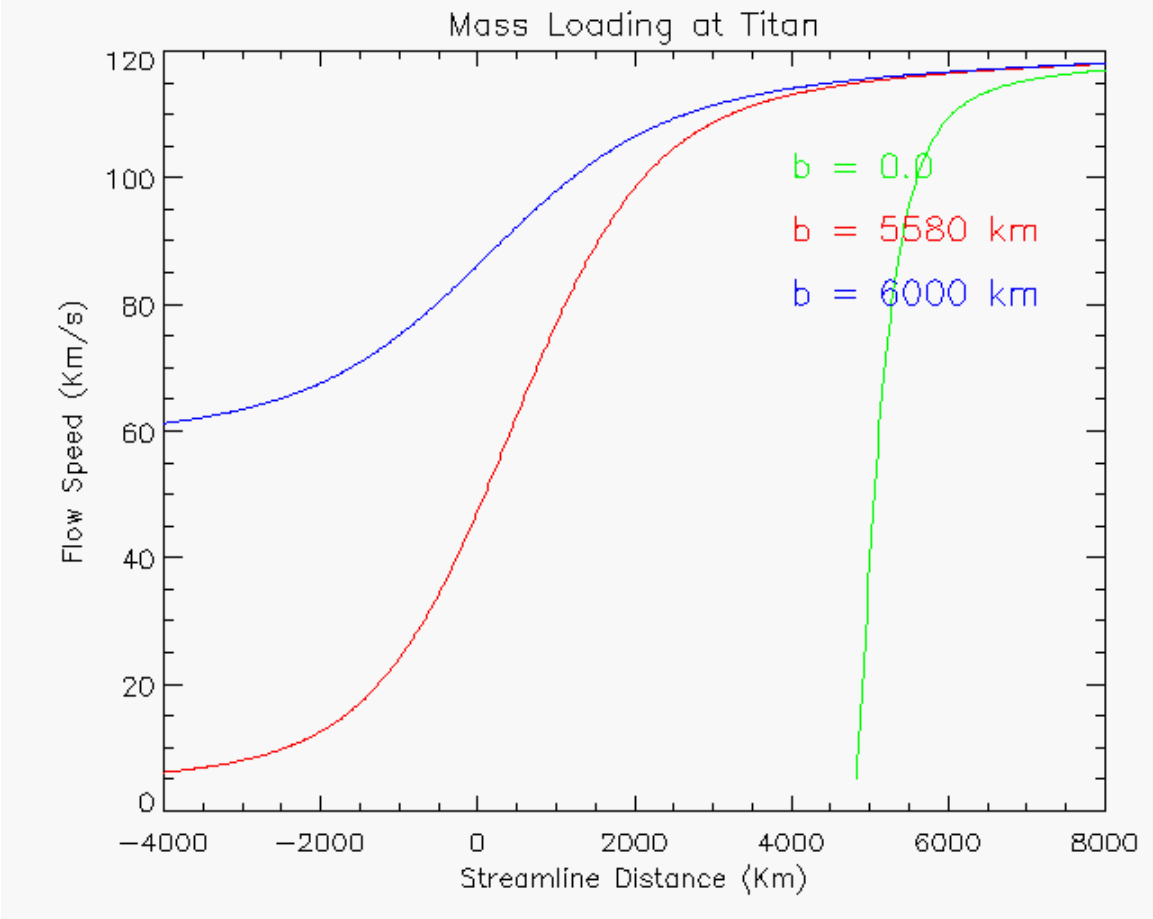
Mass Loading at Titan
b = 0.0
b = 5580 km
b = 6000 km
Flow Speed (Km/s)
Streamline Distance (Km)
120
100
80
60
40
20
0
−4000
−2000
0
2000
4000
6000
8000

Figure 6.